Two Modes of Transformation of Amorphous Calcium Carbonate Films in Air

Xurong Xu, Joong Tark Han, Do Hwan Kim, and Kilwon Cho*

Department of Chemical Engineering, Polymer Research Institute, Pohang University of Science and Technology, Pohang, 790-784, Korea

Received: October 7, 2005; In Final Form: December 14, 2005

Large-area amorphous calcium carbonate (ACC) films in air are shown to be transformed into crystalline calcium carbonate ($CaCO_3$) films via two modes—dissolution−recrystallization and solid−solid phase transition—depending on the relative humidity of the air and the temperature. Moisture in the air promotes the transformation of ACC into crystalline forms via a dissolution−recrystallization process. Increasing the humidity increases the rate of ACC crystallization and gives rise to films with numerous large pores. As the temperature is increased, the effect of moisture in the air is reduced and solid−solid transition by thermal activation becomes the dominant transformation mechanism. At 100 and 120 °C, ACC films are transformed into predominantly (110) oriented crystalline films. Collectively, the results show that calcium carbonate films with different morphologies, crystal phases, and structures can be obtained by controlling the humidity and temperature. This ability to control the transformation of ACC should assist in clarifying the role of ACC in the biomineralization of $CaCO_3$ and should open new avenues for preparing $CaCO_3$ films with oriented and fine structure.

Introduction

Calcium carbonate ($CaCO_3$) is an important mineral in nature. In addition to being an important component of sedimentary rocks, it is also a biomineral found in many organisms. The ability of organisms to control the crystallization of inorganic species is amazing. Typically, organisms synthesize complex and fine $CaCO_3$-based structures by cooperation between organic macromolecules and the inorganic species undergoing crystallization.[1] By mimicking this process, researchers have synthesized $CaCO_3$ by combining soluble macromolecules with functional insoluble matrixes.[2] The oriented growth of $CaCO_3$ crystals on various functional templates, including Langmuir monolayers[3] and self-assembled monolayers (SAMs)[4] supported on gold or silver, has been widely studied.

Amorphous calcium carbonate (ACC), a metastable form of calcium carbonate, is widely found in organisms and in vitro,[5−17] where it plays an important role in the biomineralization and crystallization of $CaCO_3$.[5,15] Despite its importance, however, previous studies have tended to overlook ACC due to its low stability and high solubility. Recent findings showing that ACC is a precursor of crystalline $CaCO_3$ and of a form of $CaCO_3$ with a complex hybrid structure have heightened interest in ACC.[9,12−19] The rich variety of $CaCO_3$ structures in nature may be due to the amorphous character of ACC, which enables it to be easily molded into many different shapes. Thus, in work on biomineralization, it is essential to study the mechanism by which ACC is transformed; the knowledge gleaned from such studies can then be used to control its transformation.

The transformation of vaterite or aragonite into calcite has been well studied.[20] Two mechanisms have been proposed for this transformation: solid-state transformation[21] and dissolution−recrystallization.[11a,11b,20] By contrast, the transformation of ACC into crystalline $CaCO_3$ has received little attention.[11a,11b,18,19] Recently, Addadi et al.[5] have demonstrated the existence of transient forms and stable forms of biogenic ACC. Li and Mann[18,19] used water to induce mesoscale transformation of surfactant-stabilized ACC in a reverse microemulsion and found that the extent of water penetration into the ACC cores was important to the formation of a complex hybrid structure. Aizenberg et al.[16] fabricated single-crystalline calcite on an imprinted substrate through the transformation of ACC in solution.

Previously[15a] we successfully prepared large-area ACC films by intercepting the crystallization process of $CaCO_3$ in solution and directly observed the transformation of these ACC films into crystalline $CaCO_3$ in air. We also used polymer templates to fabricate mosaic, single-crystal $CaCO_3$ thin films from ACC films[15b] and to study the effect of polymer chain mobility and functionality on the transformation of ACC films.[15c] The findings of those studies[3d,15] suggested that $CaCO_3$ crystallizes via a multistep process and led us to speculate that it should be possible to control the morphology, structure and crystal orientation of $CaCO_3$ by varying the system conditions so as to control the stability and transformation process of ACC. The ability to control the transformation of ACC would assist in clarifying the role of ACC in the biomineralization of $CaCO_3$ and would open new avenues for preparing $CaCO_3$ films with oriented and fine structure. Moreover, large-area ACC films can be used to study the controlled transformation of ACC in detail. In the present study, we examined the transformation of large-area ACC films into crystalline films in air as a function of temperature and the relative humidity (RH) of the air.

Experimental Section

Substrate. Silicon wafers were cleaned by immersion in freshly prepared piranha solution (concentrated H_2SO_4: H_2O_2 = 7:3, w/w) and heated for 1 h at 100 °C, then rinsed thoroughly with distilled water.

* To whom correspondence should be addressed. E-mail: kwcho@postech.ac.kr. Fax: +82-54-279-8269. Tel: +82-54-279-2270.

10.1021/jp055712w CCC: $33.50
Published on Web 01/25/2006

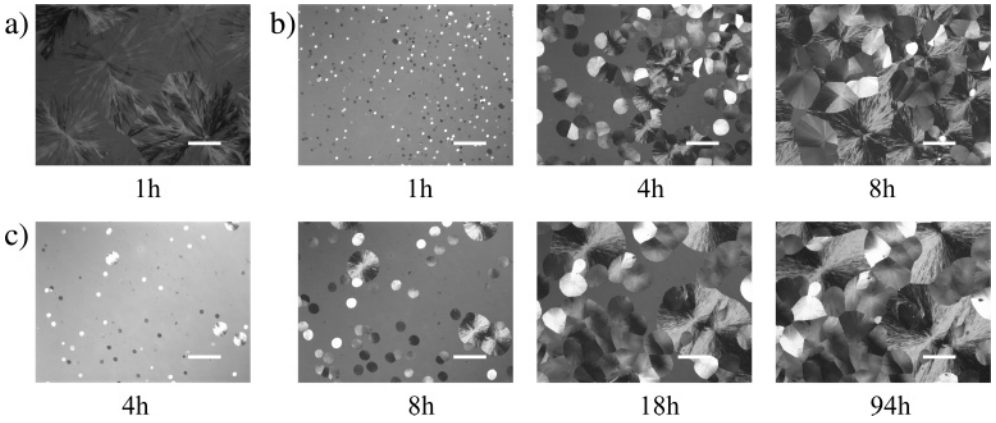

Figure 1. Optical microphotographs of ACC films at different crystallization time under three humidity conditions, respectively: (a) under high RH (90 ± 10%); (b) under medium RH (60 ± 10%); (c) under low RH (35 ± 3%). The scale bar is 100 μm.

Film Preparation[15a] and Transformation. A vial (about 25 mL) filled with 50 mM calcium chloride ($CaCl_2$) solution was placed in a desiccator along with a dish containing 6 g of ammonium carbonate [$(NH_4)_2CO_3$] powder. Clean substrate was placed upside down on top of the $CaCl_2$ solution. A thin film of $CaCO_3$ was deposited onto the substrate by slow diffusion of the CO_2 produced by decomposition of $(NH_4)_2CO_3$ at room temperature. The deposition time was 50 min. After deposition, the film was rinsed with ethanol and dried using nitrogen gas. The film was then immediately transferred to an environment with the desired humidity and temperature for the crystallization experiment.

Three humidity conditions were used: low RH (35 ± 3%); medium RH (60 ± 10%), and high RH (90 ± 10%). The low and medium RH conditions were achieved by introducing nitrogen into the chamber along with a bottle of water. The high RH condition (90 ± 10%) was achieved by placing a bottle of water in a closed chamber. The humidity was determined using a humidity meter. The experiments varying the humidity were all carried out at room temperature (22 ± 2 °C). The transformation of ACC at different temperature was investigated by immediately transferring the ACC films dried by nitrogen gas to the hot stage at the desired temperature in air.

Preparation of ACC Powder. Hydrolysis of dimethyl carbonate catalyzed by sodium hydroxide was used to prepare ACC powder, according to method 1 (excess of dimethyl carbonate) of Wegner et al.[17] ACC powder was dried under vacuum. After dried under vacuum, a part of ACC powder was treated for 48 h at 80 °C in air.

Characterization. Optical microscopy (OM, Ziess) and IR spectroscopy were used to monitor the crystallization process. For scanning electron microscopic examination, samples were Pt-coated and examined using a Hitachi S-4200 field emission scanning electron microscope (FE-SEM) with an operating voltage of 8 kV. Tapping mode images were obtained using a Multimode Nanoscope IIIa (Digital instruments). For IR spectroscopy analysis, the films on silicon wafers were scanned from 4000 to 400 cm^{-1} in transmission mode (FT-IR, BIO-RAD FTS375C). A cleaned silicon wafer was used as a reference. Differential scanning calorimetry (DSC) and thermogravimetric analysis (TGA) measurements were performed at 10 K/min on Perkin-Elmer DSC 7 and on TGA 2050 (TA Instrument) under nitrogen gas, respectively. X-ray diffraction (XRD) studies (reflection mode) were performed using a synchrotron X-ray radiation source (3C2 beamline, wavelength 1.598 Å) at the Pohang Accelerator Laboratory, Pohang, Korea.

Results

The Effect of Humidity. Here, large-scale ACC films were prepared by the method outlined in our previous paper.[15a] To test the effect of humidity on the transformation of ACC films in air, ACC films were transformed into crystalline films under three humidity conditions. Figure 1 shows optical microphotographs of ACC films at different crystallization times under the three humidity conditions. Under high RH, the ACC film had transformed into crystalline film after only 1 h (Figure 1a). When the ACC film was crystallized under medium RH, isolated small crystals appeared in the film at 1 h, which grew continuously to form slightly bigger crystals by 4 h and completely covered the film by 8 h (Figure 1b). Under low RH, by contrast, only small crystals were observed after 4 h, the film was not fully covered by crystals after 8h, and some ACC was still evident even after 18 h (Figure 1c). The present experiments thus show that the rate of ACC crystallization increases with increasing RH.

There are three anhydrous crystalline polymorphs of $CaCO_3$ (vaterite, aragonite, and calcite) and three metastable forms (ACC and crystalline monohydrate and hexahydrate $CaCO_3$). Each of these forms of $CaCO_3$ has distinct IR spectral characteristics; hence FT-IR is a powerful tool for characterizing ACC and monitoring its transformation. Figure 2 shows the IR spectra of ACC films at different crystallization times under the three humidity conditions. In the IR spectra of the as-deposited ACC films, the absorption bands are quite broad, consistent with an amorphous structure. These spectra exhibit a broad water absorption band at around 3400 cm^{-1}, a pair of split peaks at 1470 and 1408 cm^{-1} (ν_3), and the carbonate out-of-plane bending absorption at around 866 cm^{-1} (ν_2). The crystallization of these ACC films was easily monitored by observing the changes in the characteristic absorption bands, in particular the water absorption band and the ν_2 absorption band of carbonate. After the ACC film had been kept under high RH for only 1 h, the water absorption band had almost disappeared and the ν_2 absorption band of carbonate had shifted from 863 to 875 cm^{-1} and had become narrower. After 4 h under medium RH, the water absorption band had decreased in intensity and the ν_2 absorption band of carbonate had begun to shift. After 8 h under medium RH, the water absorption band had almost disappeared and the ν_2 absorption peak of carbonate was very narrow. Under low RH, however, the IR spectra of the ACC film did not show changes indicative of transformation and crystallization until about 18 h. Even at 18 h, a quite strong and broad water absorption band was still evident in the IR spectrum, indicating that some ACC remained in the film. These

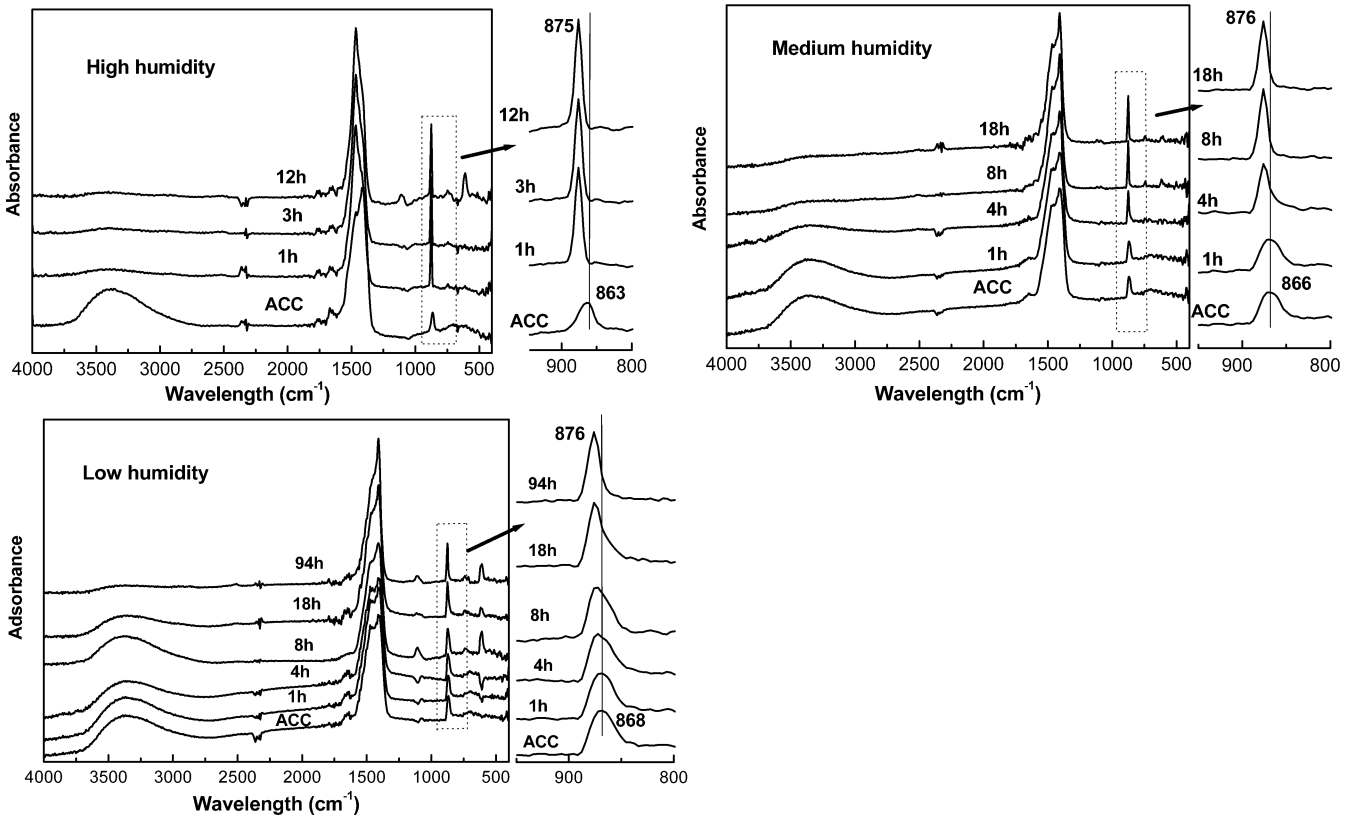

Figure 2. IR spectra of the transformation process of ACC films into crystalline films under three humidity conditions, respectively.

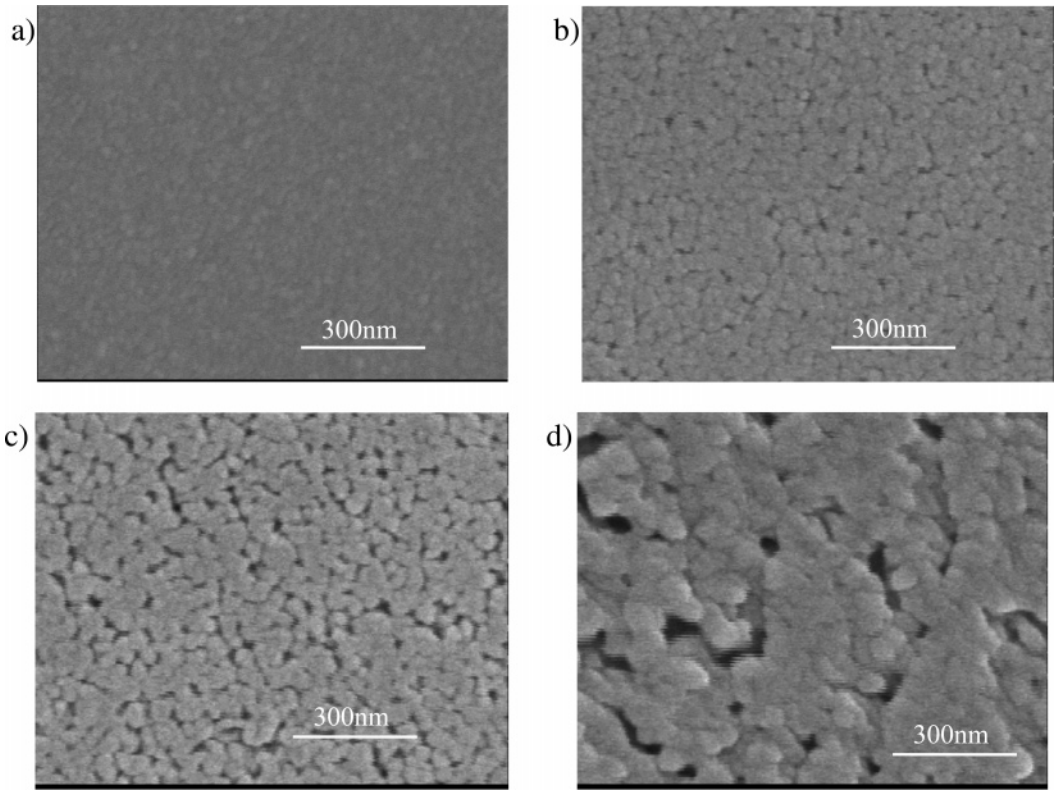

Figure 3. SEM micrographs of $CaCO_3$ films (a) ACC and after finished to crystallize under relative humidities of (b) 35 ± 3%, (c) 60 ± 10%, and (d) 90 ± 10%.

results are in good accord with the optical microscopy results presented above (Figure 1).

We next used SEM to analyze the morphology and structure of the $CaCO_3$ films crystallized under different ambient humidity. The SEM micrograph of the as-deposited ACC film (Figure 3a) shows no apparent structure other than some indistinct nanoparticles. However, the SEM micrographs of the surfaces after complete crystallization of the films under low RH (Figure 3b), medium RH (Figure 3c), and high RH (Figure 3d) are dramatically different and reveal very interesting morphologies.

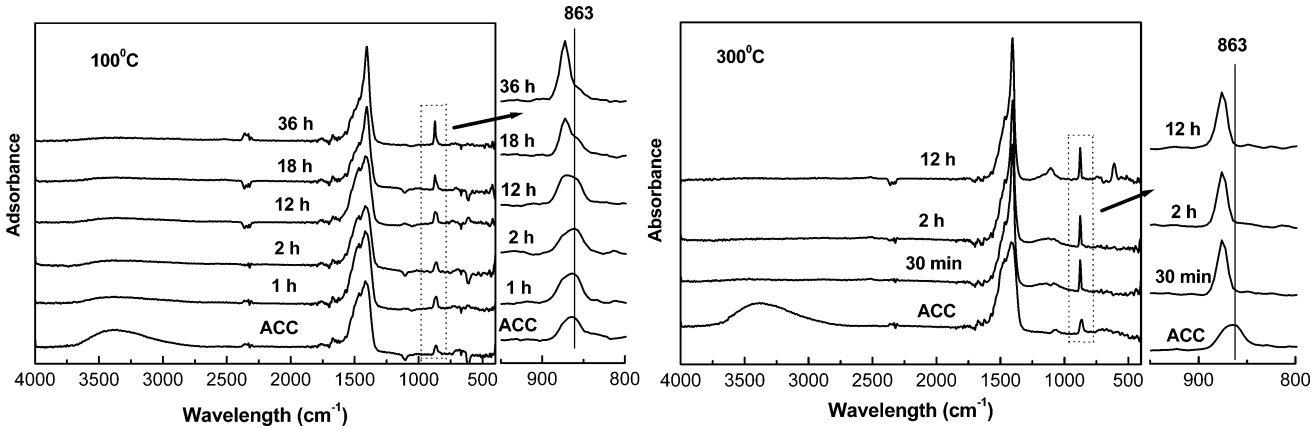

Figure 4. IR spectra of the transformation process of ACC films into crystalline films at 100 and 300 °C.

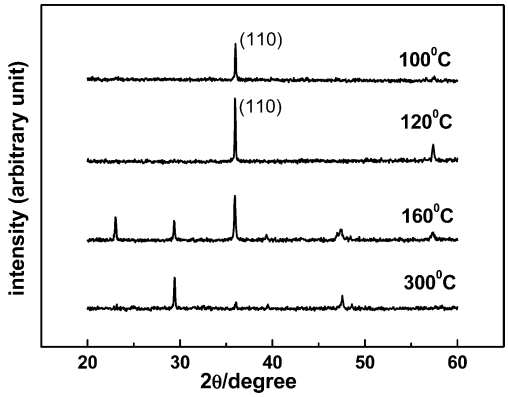

Figure 5. XRD data of $CaCO_3$ films crystallized under different temperatures.

The most prominent feature of all of these crystallized surfaces is the presence of numerous pores. However, the pore area and depth increase with increasing humidity. Additionally, it seems that higher humidity induces better coalescence between $CaCO_3$ nanoparticles.

The Effect of Temperature. The transformation of ACC into crystalline forms can also be thermally activated. To examine this behavior, ACC films were crystallized at 100, 120, 160, or 300 °C. As for the humidity test, the transformation processes was monitored by FT-IR spectroscopy. The IR spectra recorded at 100 and 300 °C are shown in Figure 4. After only 30 min at 300 °C, the water absorption band of ACC had disappeared and the ν_2 out-of-plane absorption peak of carbonate had shifted from 863 to 875 cm^{-1} and become narrower, indicating the rapid transformation of ACC into a crystalline form. After 1 h at 100 °C, by contrast, the strength of the water absorption band of ACC around 3400 cm^{-1} had decreased, but the ν_2 absorption peak of carbonate had remained unchanged. Even after 12 h, the ν_2 absorption peak of carbonate had only begun to differ slightly from that of ACC. After 36 h, the ν_2 absorption peak of carbonate had shifted and become narrower.

XRD data (Figure 5) indicated that calcite films were formed at all temperatures. An interesting aspect of the X-ray data (Figure 5) is that the (110) orientation is favored at 100 and 120 °C and, to lesser extent, at 160 °C, but at the higher temperature of 300 °C, the crystal shows no preferred orientation. Thus, as the crystallization temperature was increased, the calcite films formed by the crystallization of ACC films gradually changed from oriented to unoriented films.

Crystallized films from thermally activated ACC are characterized by low roughness and contrast of the surfaces, making it difficult to extract information using SEM. Hence, in the present study we used AFM to characterize the surface morphologies of the films. The AFM height and phase images of the ACC film before crystallization (Figure 6a) clearly show many nanoparticles on the film surface, consistent with the SEM finding (Figure 3a). After crystallization at 100 °C (Figure 6b), the nanoparticle morphology disappears and a new, well-organized structure is observed that lacks the pores observed on the films crystallized under low, medium, and high RHs at room temperature. However, the AFM images of the film crystallized at 300 °C (Figure 6c) are dramatically different from those of the film crystallized at 100 °C; specifically, the 300 °C images resemble the AFM images of the original ACC film (Figure 6a). The AFM results therefore indicate that during crystallization at 300 °C, the ACC nanoparticles are transformed into crystalline nanoparticles in a process that maintains the shape of the nanoparticles. This structure resembles that reported recently by Li et al.,[22] who showed that individual aragonite

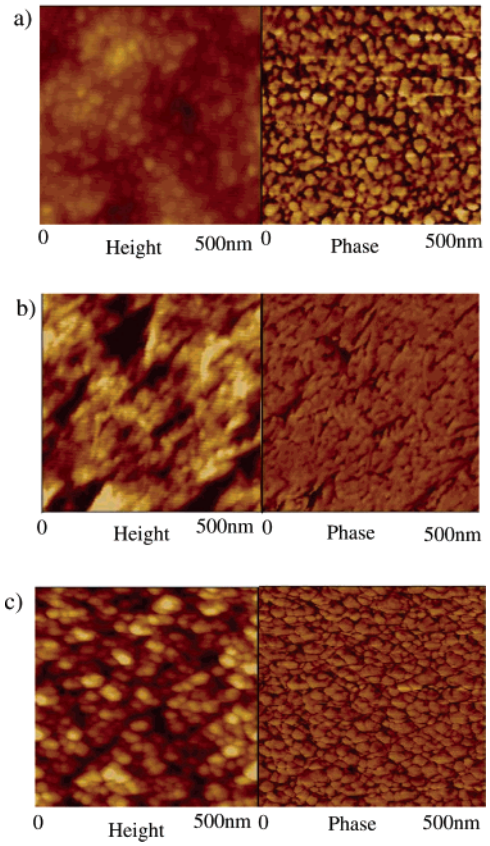

Figure 6. AFM images: (a) ACC film; (b) $CaCO_3$ film crystallized at 100 °C; (c) $CaCO_3$ film crystallized at 300 °C.

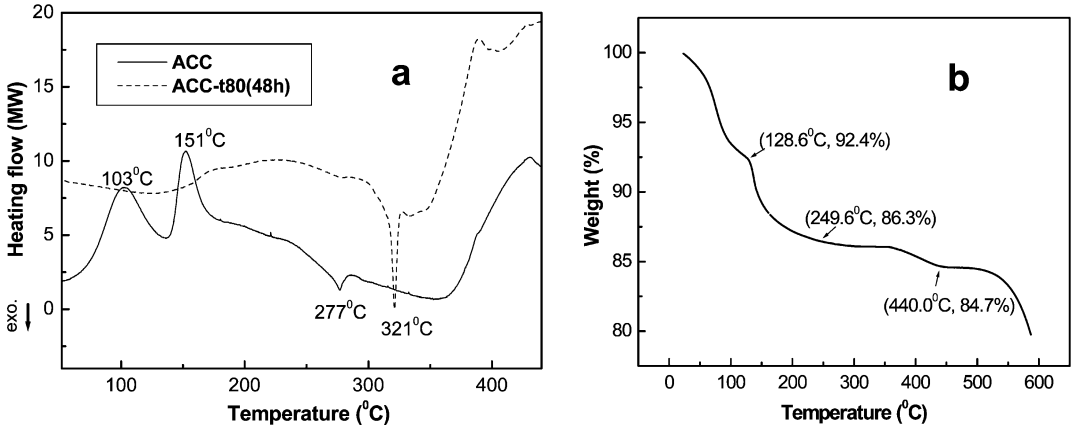

Figure 7. (a) DSC curves of ACC (solid line) and ACC heated at 80 °C for 48 h (dash line), heating rate 10K/min, N_2 atmosphere; (b) TGA curve of ACC at heating rate 10 K/min.

platelets of nacre are composed of numerous cobblelike polygonal nanograins.

To clarify the thermally activated transformation of ACC,[23] we synthesized ACC powder[17] and studied its thermal behavior by DSC and TGA measurement (Figure 7). Two endothermic processes (peaks at 103 and 151 °C) and one exothermic process (peaks at 277 °C) were observed on the DSC thermogram (Figure 7a) of the as-received ACC. The two endothermic processes correspond to the two steps of weight loss on TGA curve (Figure 7b) and can be contributed to the release of water included in the ACC. The observation of two such peaks indicates that the water in ACC exists in two environments, with different strengths of interaction with the ACC. The exothermic process at 277 °C corresponds to transformation of disordered ACC into ordered $CaCO_3$ crystals, whose enthalpy change ΔH is −0.86 kJ/mol. However, if ACC was preheated for 48 h at 80 °C, the endothermic processes became broader and the endothermic peak weakened and shifted to higher temperature (Figure 7a), while the exothermic peak simultaneously shifted to higher temperature and a larger enthalpy change appeared.

Discussion

It is commonly accepted that ACC is a highly unstable polymorph of $CaCO_3$ that readily crystallizes. The present results indicate that humidity significantly affects the transformation of ACC at room temperature. Specifically, the rate of transformation of ACC at room temperature increases with increasing RH. Furthermore, the final morphology of the $CaCO_3$ film surface, in particular the porosity, depends on the transformation conditions. This ability to control the porosity of the $CaCO_3$ film surface by varying the crystallization conditions could potentially be useful in the papermaking industry or in catalyst carrier applications. Despite the reputation of ACC as unstable, actually, ACC films can be kept under vacuum at room temperature for more than 3 months without showing evidence of crystallization, indicating that ACC is quite stable at room temperature under dry conditions.

Aizenberg et al.[16] suggested that the crystallization of $CaCO_3$ in solution occurs via mass transport between the amorphous and crystalline phases, that is, via a dissolution−recrystallization process.[10a] This picture can be extended to our experiments in air. Dissolution−recrystallization involves the dissolution of ACC in solution and the crystallization of ACC into one of its crystalline form from solution, leading to a change in the morphology of ACC film. It can be suggested that water in ambient humid air is adsorbed on the surface of ACC and induces the dissolution of ACC to form a saturated solution of ACC. Since the solubility of ACC is higher than anhydrous crystalline forms, the saturated solution of ACC is supersaturated for anhydrous calcium carbonate crystalline forms. The saturated solution of ACC is an unstable thermodynamic system so that calcium carbonate crystals will spontaneously nucleate and grow from it. Thus, given that water promotes the dissolution−recrystallization process of $CaCO_3$, increasing the humidity would be expected to induce and speed up the transformation of ACC by supplying a matrix in which it can dissolve and recrystallize. This, in turn, will lead to the formation of larger pores and to better coalescence and reorganization of ACC nanoparticles. The findings presented here are consistent with this picture. Therefore, the present results indicate that the humidity of the air in contact with an ACC film plays an important role in the transformation of the ACC and that it is possible to control the structure, polymorph, and morphology of $CaCO_3$ films formed in air by controlling the humidity.

When the ACC film is heated to high temperature, the crystallization mechanism is expected to be determined by the increased thermal energy rather than the air humidity. Increasing the temperature will promote the transformation of ACC by supplying more energy, which will allow the ionic species in ACC to cross the energy barrier for realignment. The transformation of an amorphous ionic solid into a crystalline one is a very complicated process, which may involve the formation of some metastable intermediate phase.[24,25]

In our experiments, $CaCO_3$ films crystallized at 100 and 120 °C showed a predominant (110) orientation, whereas no predominant orientation was observed in the $CaCO_3$ film crystallized at 300 °C, and a $CaCO_3$ film with intermediate structure was obtained at 160 °C. In contrast to the thermal behavior of ACC, the temperatures of 100 and 120 °C are located in the temperature range of the first endothermic process in the DSC thermogram (Figure 7) and below the temperature range of the second endothermic process. The temperature of 160 °C lies in the temperature range of the second endothermic process. However, the highest temperature considered, 300 °C, is higher than the peak temperature of the exothermic process, and induces rapid dehydration and crystallization of ACC such that the nanoparticle morphology remains almost unchanged (Figure 6c). The $CaCO_3$ film formed after crystallization at 300 °C showed no predominant orientation. Taken together, our DSC and IR spectral data indicate that heating ACC at 100 and 120 °C causes the rapid release of the more weakly bound water molecules in ACC, but the more tightly bound water molecules are released only slowly, leading to long crystallization times.

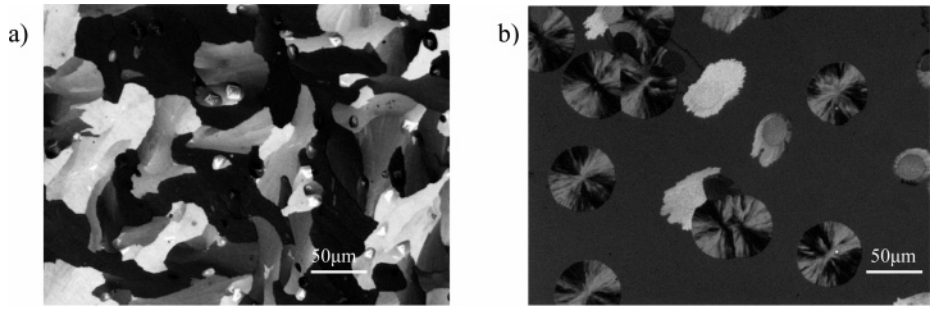

Figure 8. Optical micrograph of the $CaCO_3$ film under crossed-polarized light in reflection mode: (a) crystallized at 100 °C (after crystallized); (b) first crystallized under medium RH for 4 h at room temperature, then heated at 100 °C for 12 h in air (not completely crystallized).

An atomistic simulation approach[26] has shown that the surface energy of calcite (104) surfaces is lowest among all crystal surfaces and the (110) surface has a little higher surface energy. However, the effect of molecular adsorption of water onto the calcite (110) crystal surface on its surface energy is more significant than that on (104) crystal surface[26] and that the molecular adsorption of water onto the calcite (110) crystal surface greatly stabilizes the (110) crystal face. The presence of water molecules within the transforming $CaCO_3$ films at 100 and 120 °C and the longer crystallization time may promote the formation of predominantly (110) oriented $CaCO_3$ films, although the detailed mechanism remains unknown.

The above results indicate that ACC is transformed into crystalline $CaCO_3$ via two modes: dissolution−recrystallization[10a,15] and solid−solid phase transition.[5] At room temperature, moisture in the air promotes the transformation of ACC into crystalline forms via the dissolution−recrystallization mechanism and spherulites are usually obtained in the film (Figure 1). As the temperature is increased, however, the effect of moisture in the air is reduced and solid−solid transition by thermal activation becomes the dominant transformation mechanism, giving rise to mosaic polycrystalline films (Figure 8a). Thus, by varying the treatment conditions, a range of structures can be obtained, including different crystalline polymorphs and oriented and unoriented structures. For example, an ACC film that is first crystallized under medium RH at room temperature for 4 h, and then incubated at 100 °C for 12 h in air, gives a film with the structure shown in the optical micrograph in Figure 8. When subjected to these conditions, the ACC does not completely transform into crystalline phase; rather, two morphologies, spherulites formed under medium RH and mosaic crystals formed at 100 °C, can be clearly seen.

The transformation of vaterite or aragonite into calcite in water through a dissolution−recrystallization process has been well established. Sawada et al.[10a,10b] and Aizenberg et al.[15] suggested that ACC would also transform into a crystalline phase by a dissolution−recrystallization process in solution. However, Addadi et al.[5,10] have described two types of ACC, stable hydrous ACC and transient anhydrous ACC, which contains small domains of structural order. Importantly, the structural order in the ordered domains in the transient anhydrous form of ACC was found to resemble the crystalline form into which the ACC is ultimately transformed.[8] On the basis of this observation, Addadi et al. proposed that the crystallization of ACC may proceed via a solid−solid phase rearrangement in which these domains of short-range order align and coalesce.[5] Their results were mainly derived from studies of biogenic ACC. However, here we have established that two types of synthetic ACC can be obtained, as shown in the DSC analysis (Figure 7a). Furthermore, the enthalpy change (ΔH) for the transformation of disordered ACC into ordered $CaCO_3$ crystals of as-received ACC and of ACC after treated at 80 °C are −0.86 and −2.49 kJ/mol, respectively. Both of these ΔH values are sufficiently small[27] that the thermodynamic energy barrier of the solid−solid transformation process can be easily crossed. It is possible to imagine that organisms have evolved such that they exploit the variable biomineralization behavior of ACC to assemble desirable complicated but fine structures with appropriate crystal phases by dissolution−recrystallization or solid−solid transformation at the lowest energy cost.

To date, however, the low stability and high solubility of ACC have made it difficult to examine the transformation of ACC in solution in detail, despite the existence of stable forms of ACC in organisms.[5] The ability to easily prepare large-area ACC films[14] provides an excellent opportunity to elucidate the mechanisms involved in the crystallization and biomineralization of $CaCO_3$. Additionally, in organisms, the template strategy is extensively adopted to control the oriented structure, morphology, and polymorph of $CaCO_3$ biominerals. Polymers,[2] Langmuir monolayers,[3] and SAMs[4] have been used as templates to mimic the formation of $CaCO_3$ in biological systems. Although ACC has previously been overlooked due to its high solubility and low stability, this amorphous phase plays important roles in the crystallization and biomineralization of $CaCO_3$.[5,14] Indeed, the results presented here show that it is possible to control the oriented structure, morphology, and polymorph of $CaCO_3$ films by controlling the transformation of ACC without the aid of templates.

Conclusion

We observed two modes of transformation of ACC in air into ordered structures: dissolution−recrystallization and solid−solid phase transition. In addition, we found that oriented large-area calcite films could be prepared by controlling the transformation of an ACC film by varying the air humidity and temperature conditions in air, without the aid of a functional template. Under conditions of high humidity, ACC tends to dissolve and recrystallize, whereas at high temperatures, ACC is transformed into the crystalline form via a solid−solid transition. The modes for controlling the transformation of ACC described here could potentially be exploited to create $CaCO_3$ films with fine structures under simple and mild conditions.

Acknowledgment. This work was supported by a Grant (No. 04K1501-01310) from the Center for Nanostructural Materials Technology under the 21st Century Frontier R&D Programs of the Ministry of Science and Technology, the National Research Laboratory Program and ERC Program (R11-2003-006-03005-0) of the MOST/KOSEF, and the Brain Korea 21 Program of the Ministry of Education and Human Resources Development of Korea.

References and Notes

(1) (a) Mann, S.; Webb, J.; Williams, R. J. P. *Biomineralization: Chemical and biochemical Perspectives*; VCH Publishers: New York, 1989; (b) Mann, S. *Biomineralization: principles and concepts in bioinorganic materials chemistry*; Oxford University Press: New York, 2001; (c) Meldrum F. C. *Int. Mater. Rev.* **2003**, *48*, 187.

(2) (a) Kato, T.; Suzuki, T.; Amamiya, T.; Irie, T.; Komiyama, M., Yui, H. *Supramol. Sci.* **1998**, *5*, 411; (b) Kato, T.; Sugawara, A.; Hosoda, N. *Adv. Mater.* **2002**, *14*, 869; (c) Hosoda, N.; Kato, T. *Chem. Mater.* **200**1, *13*, 688; (d) Sugawara, A.; Ishii, T.; Kato, T. *Angew. Chem., Int. Ed.* **2003**, *42*, 5299; (e) Zhang, S. K.; Gonsalves, K. E. *Mater. Sci. Eng.* **1995**, *C3*, 117; (f) Zhang S. K.; Gonsalves, K. E. *Langmiur* **1998**, *14*, 6761. (g) Ajikumar, P. K.; Lakshminarayanan, R.; Valiyaveettil, S. *Cryst. Growth Des.* **2004**, *4*, 331−335; (h) Lakshminarayanan, R.; Valiyaveettil, S.; Loy, G. L. *Cryst. Growth Des.* **2003**, *3*, 953. (i) Falini, G.; Fermani, S.; Gazzano, M.; Ripamonti, A. *Chem.−Eur. J.* **1997**, *3*, 1807.

(3) (a) Mann, S.; Heywood, B. R.; Rajam, S.; Birchall, J. D. *Nature* **1988**, *334*, 692; (b) Heywood, B. R.; Mann, S. *Adv. Mater.* **1994**, *6*, 9; (c) Heywood, B. R.; Rajam, S.; Mann, S. *J. Chem. Soc., Faraday Trans.* **1991**, *87*, 735; (d) Xu, G. F.; Yao, N.; Aksay, I. A.; Groves, J. T. *J. Am. Chem. Soc.* **1998**, *120*, 11977.

(4) (a) Küther, J.; Seshadri, R.; Knoll, W.; Tremel, W. *J. Mater. Chem.* **1998**, *8*, 641; (b) Aizenberg, J.; Black, A. J.; Whitesides, G. M. *Nature* **1998**, *394*, 868; (c) Aizenberg, A. J. Black, G. M. Whitesides, *Nature* **1999**, *398*, 495; (d) Aizenberg, J.; Black, A. J.; Whitesides, G. M. *J. Am. Chem. Soc.* **1999**, *121*, 4500. (e) Han, Y. J.; Aizenberg, J. *Angew. Chem., Int. Ed.* **2003**, *42*, 3668.

(5) Addadi, L.; Raz, S.; Weiner, S. *Adv. Mater.* **2003**, *15*, 959.

(6) (a) Politi, Y.; Arad, T.; Klein, E.; Weiner, S.; Addadi, L. *Science* **2004**, *306*, 1161; (b) Weiner, S.; Levi-Kalisman, Y.; Raz, S. *Connect. Tissue Res.* **2003**, *44*, 214 (Suppl. 1).

(7) Beniash, E.; Aizenberg, J.; Addadi, L.; Weiner, S. *Proc. R. Soc. London, Ser. B* **1997**, *264*, 461.

(8) Hasse, B.; Ehrenberg, H.; Marxen, J.; Becker, W.; Epple, M. *Chem.−Eur. J.* **2000**, *6*, 3679.

(9) Gower, L. B.; Odom, D. J. *J. Cryst. Growth* **2000**, *210*, 719.

(10) Raz, S.; Hamilton, P. C.; Wilt, F. H.; Weiner, S. Addadi, L. *Adv. Funct. Mater.* **2003**, *13*, 480.

(11) (a) Sawada, K. *Pure Appl. Chem.* **19**97, *69*, 921; (b) Ogino, T.; Suzuki, T.; Sawada, K. *Geochim. Cosmochim. Acta* **1987**, *51*, 2757; (c) Brečević, Lj.; Nielsen A. E. *J. Cryst. Growth* **1989**, *98*, 504; (d) Clarkson, J. R.; Price, T. J.; Adams, C. J. *J. Chem. Soc., Faraday Trans.* **1992**, *88*, 243.

(12) (a) Donners, J. J. J. M.; Nolte, R. J. M.; Sommerdijk, N. A. J. M. *J. Am. Chem. Soc.* **2002**, *124*, 9700; (b) Donners, J. J. J. M.; Heywood, B. R.; Meijer, E. W.; Nolte, R. J. M.; Sommerdijk, N. A. J. M. *Chem.−Eur. J.* **2002**, *8*, 2561.

(13) Dimasi, E.; Patel, V. M.; Sivakumar, M.; Olszta, M. J.; Yang, Y. P.; Gower, L. B. *Langmuir* **2002**, *18*, 8902.

(14) Loste, E.; Meldrum, F. *Chem. Commun.* **2001**, 901.

(15) (a) Xu, X. R.; Han, J. T.; Cho, K. *Chem. Mater.* **2004**, *16*, 1740; (b) Han, J. T.; Xu, X. R.; Kim, D. H.; Cho., K. *Adv. Funct. Mater.* **2005**, *15*, 475; (c) Han, J. T.; Xu, X. R.; Kim, D. H.; Cho., K. *Chem. Mater.* **2005**, *17*, 136.

(16) Aizenberg, J.; Muller, D. A.; Grazul, J. L.; Hamann, D. R. *Science* **2003**, *299*, 1205.

(17) Faatz, M.; Gröhn, F.; Wegner, G. *Adv. Mater.* **2004**, *16*, 996.

(18) Li, M.; Lebeau, B.; Mann, S. *Adv. Mater.* **2003**, *15*, 2032.

(19) Li, M.; Mann, S. *Adv. Funct. Mater.* **2002**, *12*, 773.

(20) (a) Nancollas, G. H. *Biological mineralization and demineralization*; Springer-Verlag: 1982; p 70; (b) Ogino, T.; Suzuki, T.; Sawada, K. *J. Cryst. Growth* **1990**, *100*, 159; (c) Perić, J.; Vučak, M.; Krstulović, R.; Brečević, Lj. Kralj, D. *Thermochim. Acta* **1996**, *277*, 175; (d) JimÉnez-López, C.; Caballero, E.; Huertas, F. J.; Romanek, C. S. *Geochim. Cosmochim. Acta* **2001**, *65*, 3219; (d) Wolf, G.; Günther, C. *J. Therm. Anal. Cal.* **2001**, *65*, 687.

(21) Nakahara, Y.; Tazawa, T.; Miyata, K. *Nippon Kagaku Kaishi* **1976**, *5*, 732.

(22) Li, X. D.; Chang, W. C.; Chao, Y. J.; Wang, R. Z.; Chang, M. *Nano. Lett.* **2004**, *4*, 613.

(23) Koga, N.; Nakagoe, Y.; Tanaka, H. *Thermochim. Acta* **1998**, *318*, 239.

(24) Noh, D. Y.; Lee, H. H.; Kang, T. S.; Je, J. H. *Appl. Phys. Lett.* **1998**, *72*, 2823.

(25) Lyahovitskaya, V.; Fildman, Y.; Zon, I.; Wachtel, E.; Gartsman, K.; Tagantsev, A. K.; Lubomirsky, I. *Phys. Rev. B* **2005**, *71*, 094205.

(26) De leeuw, N. H.; Parker, S. C. *J. Phys. Chem. B* **1998**, *102*, 2914.

(27) Navrotsky, A. *Proc. Natl. Acad. Sci. U.S.A.* **2004**, *101*, 12096.